Nanoscale

Monolayer 2D ZrTe2 transition metal dichalcogenide as nanoscatter for random laser action

Journal:	*Nanoscale*
Manuscript ID	NR-ART-04-2020-003152.R1
Article Type:	Paper
Date Submitted by the Author:	02-Jul-2020
Complete List of Authors:	Pincheira, Pablo; Universidad de La Frontera, Departamento de Ciencias Físicas Silva Neto, Manoel; Universidade Federal de Pernambuco, Física Maldonado, Melissa; Universidade Federal de Pernambuco, Física de Araújo, Cid Bartolomeu; Universidade Federal de Pernambuco, Física Jawaid, Ali; Air Force Research Laboratory, Materials and Manufacturing Directorate Busch, Robert; Materials and Manofacturing Directorate, Air Force Laboratories Ritter, Allyson; Air Force Research Laboratory, Materials and Manufacturing Directorate Vaia, Richard; Air Force Research Laboratory, Materials and Manufacturing Gomes, Anderson; Universidade Federal de Pernambuco, Physics Department

ARTICLE

Monolayer 2D $ZrTe_2$ transition metal dichalcogenide as nanoscatter for random laser action

Pablo I.R. Pincheira[a*], Manoel L. da Silva[b] - Neto, Melissa Maldonado[c], Cid B. de Araújo[b,c], Ali M. Jawaid[d], Robert Busch[d], Allyson J. Ritter[d], Richard A. Vaia[d] and Anderson S. L. Gomes[c*]

Received 00th January 20xx,

Accepted 00th January 20xx

DOI: 10.1039/x0xx00000x

We demonstrate random laser emission from Rhodamine 6G with ZrTe2 transition metal dichalcogenide (TMD) as nanoscatters, both in powder and 2D nanoflakes liquid suspension. The 2D semimetal ZrTe2 was synthesized by a modified redox exfoliation method to provide single layer TMD, which was employed for the first time as the scatter medium to provide feedback in an organic gain medium random laser. In order to exploit random laser emission and its threshold value, replica symmetry breaking leading to a photonic paramagnetic to photonic spin glass transition in both 2D and 3D (powder) ZrTe2 was demonstrated. One important aspect of mixing organic dyes with ZrTe2 is that there is no chemical reaction leading to dye degradation, demonstrated by operating over more than 2 hours of pulsed (5Hz) random laser emission.

Introduction

Random laser (RL) emission has been demonstrated using a wealth of different gain and scattering media, which are required elements for this unconventional coherent photon source. The gain medium plays the same role as in conventional lasers, whereas the scattering medium provides the optical feedback which, in conventional lasers, is rendered by an optical cavity. RL using organic dyes[1], semiconductors [2], quantum dots [3], polymers [4], rare earth materials [5] and biological materials [6], including human tissues [7] have been demonstrated in combination with passive scatters, such as TiO_2 [1], SiO_2 [8], Al_2O_3 [9] , WO_3 [10]. Other types of scattering materials are active materials, which can play the simultaneous role of gain and scatter: semiconductors, such as ZnO [2] or nanocrystals doped with rare-earth ions, such as Nd^{3+} [5,11]. Yet another type of scatterers are metal nano or sub-micrometer particles, such as gold or silver, which can have their plasmonic properties exploited either by themselves [12-14] or mixed with other nanoparticles [15]. All the aforementioned RLs can be considered bulk architectures, which can be designed in 3D (generally powders) or 2D (planar waveguide) format. 1D or quasi-1D random lasers have been demonstrated in random fiber lasers, which can also use a plethora of gain medium and scatters [16-19]. All the above referenced development was possible thanks to the pioneer work of Lethokhov in 1968, who first proposed the possibility of lasers with scattering feedback [20]. Reviews on random lasers and random fiber lasers can be found in refs. [11, 21-24].

Among the recent development in nanomaterials, transition metal dichalcogenides (TMDs) have played a major role due to their unique applications in optoelectronics [25], nonlinear optics[26] and biomedics[27]. The development of these advanced photonic materials has been possible due to efforts in their synthesis and characterization, as reported in [28-30]. Some nanomaterials from the 2D TMD family have already been exploited as conventional laser emitters, such as WSe_2 quantum dots [31], MoS_2,[32] and reviewed in[33]. RL emission have been reported in MoS_2/Au/ZnO operating in the near infrared [34], whereby thick-layers (200 nm) of MoS_2 flakes were excited at 488 nm and emitted around 900 nm. The random laser characterization in [34] was carried out in a confocal microscopy setup using 488 nm continuous wave laser with spot size ~1µm. Another semiconducting material, hexagonal boron nitride, was liquid phase exfoliated and employed as scattering medium for random laser action in rhodamine B emitting around 580 nm, excited by pulsed 532 nm, 3 ns, 10 Hz radiation [35].

In this letter, we employ for the first time a semi-metallic $ZrTe_2$ powder (i.e. particles from $ZrTe_2$ bulk powder) and 2D monolayer of redox exfoliated ZrTe2, as nanoscatters for random laser emission. The gain medium for this proof-of-concept experiment was Rhodamine 6G, but other gain media can be used, therefore extending the emission wavelength range. Besides the routine characterization for RL emission [21,22], we also exploited the replica symmetry breaking phenomenon as a characterization tool to

[a.] *Departamento de Ciencias Fisicas, Universidad de La Frontera, Temuco, Chile E-mail: priquelmepincheira@gmail.com.*
[b.] *Graduate Program in materials Science, Universidade Federal de Pernambuco, 50670-901, Recife-PE, Brazil.*
[c.] *Departamento de Física, Universidade Federal de Pernambuco, Av. Prof. Moraes Rego, 1235, Cidade Universitária, Recife, PE 50670-901, Brazil E-mail: anderson@df.ufpe.br*
[d.] *Materials and Manofacturing Directorate, Air Force Research Laboratories, 45433, Ohio, United States.*
† Footnotes relating to the title and/or authors should appear here.
Electronic Supplementary Information (ESI) available: [details of any supplementary information available should be included here]. See DOI: 10.1039/x0xx00000x

confirm the phase-transition from photonic paramagnetic to photonic spin glass [36]. This effect occurs due to interplay between scattering, multimode emission and gain, and the phase-transition occurs exactly on the threshold for the random laser emission [36-38]. We also verified the lasing lifetime, which is shown to be over 2 hours, with no photodegradation observed.

Experimental section

2D ZrTe2 Nanoscatterers: synthesis and characterization

Synthesis – All employed materials were commercially purchased. $ZrTe_2$ from Materion, acetonitrile (ACN) from VWR, cumene hydroperoxide (technical grade, 80%) and hydroquinone (reagent grade, 99%) both from Sigma Aldrich. ACN was distilled under nitrogen and properly stored (activated molecular sieves) to prevent moisture accumulation.

Exfoliation of ZrTe2 - ZrTe2 was exfoliated via the redox exfoliation method previously described in detail in ref. [30]. Redox exfoliation proceeds via generation of polyoxometalates in-situ that adsorb to the bulk powder and facilitate delamination via coloumbic repulsion. The redox cycle allows for controlled in-situ generation of the exfoliant. In short, 10 mmol $ZrTe_2$ (3500 mg) 50 mL acetonitrile, and 500 µL cumene hydroperoxide was added to a 100 mL round bottom flask equipped with a stir bar under an inert argon atmosphere. The reaction was stirred at 50 °C. Afterwards, a solution of hydroquinone (1 mmol in 10 mL acetonitrile) was added dropwise to the solution, and allowed to stir for 30 minutes at 40 °C. The reaction was transferred to a shear mixer (IKA USA) and allowed to exfoliate for 300 minutes at 10,000 rpm. The slurry was then transferred to a centrifuge tube and exfoliated and bulk flakes were sediment at 9,000 rpm (8,500 g) for 30 minutes. The supernatant containing excess oxidant and reductant was discarded and fresh anhydrous acetonitrile (50 mL) was added to the pellet. The slurry was briefly mixed via a vorticer, and centrifuged again at 9,000 rpm (8,500 g) for 30 minutes. This process was performed a total of three times to ensure complete removal of reagents.

Monolayer Size Selection and morphological characterization of $ZrTe_2$ - The cleaned slurry containing bulk and exfoliated $ZrTe_2$ was centrifuged at 400 rpm for 3 hours. The supernatant containing exfoliated $ZrTe_2$ was collected and subjected to another round of centrifugation at 500 rpm for 3 hours. The supernatant was collected, and subsequently centrifuged at 700 rpm for 3 hours. The light olive color solution was extracted and AFM (Bruker Corporation) was performed to verify monolayer selection. Further characterization of the samples included high resolution transmission electron microscopy (HRTEM, aberration corrected FEI Talos TEM with an accelerating voltage of 200 kV), X-ray photoelectron spectroscopy (SSI XPS System), Raman spectroscopy (Renishaw) and UV-Vis spectra of exfoliated samples were measured on a Cary 5000Spectrometer. Figure 1 (a-c) shows the AFM results where the monolayer nanoflakes dimensions can be seen and FFT of the nanoflakes from SEM images.

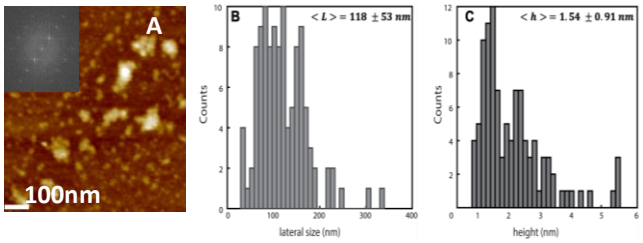

FIG. 1 Morphology of exfoliated $ZrTe_2$. AFM (a) of monolayer selected $ZrTe_2$. Inset in (a) shows the FFT from high-resolution TEM lattice imaging of an exfoliated monolayer. SEM-determined lateral size (b) and AFM-determined height (c) distributions reflect the structural disparity within the monolayer selected $ZrTe_2$. Note, the average height reported via AFM analysis is typically larger than the absolute particle size due to substrate-flake interactions.

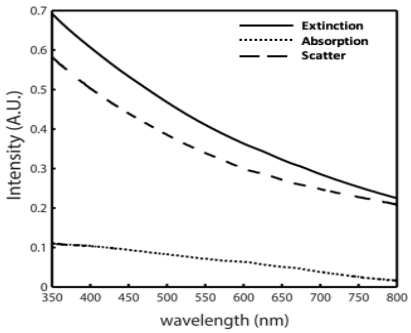

FIG.2 UV-VIS spectroscopy was performed on $ZrTe_2$ dispersions in acetonitrile (5 µg/ml). the extinction and absorbance values were measured, and extraction of the scattering profile was obtained via extinction (λ) –absorption (λ) = scatter (λ). Note that, due to the metallic nature of $ZrTe_2$, the absorption curves are featureless.

Figure 2 shows the UV-Vis spectroscopy results. The scattering profiles (dashed curves) were obtained by subtracting the extinction spectra (heavy line) from the absorbance spectra (dotted line), where Ext(λ) = Abs(λ) + Sca(λ). It is important to note that, due to the metallic nature of $ZrTe_2$, the absorption curve is featureless.

Random laser operation and characterization

Two random laser devices employing scatters with different dimensionality where prepared using Rhodamine 6G (Rh6G 10^{-4} M) in solution of ACN. First, traditional 3D scatters consisting of bulk $ZrTe_2$ powders were suspended in ACN under vigorous stirring in a concentration of 35 µg/ml. On the other hand, 2D nanoscatters consisting of redox exfoliated monolayers of $ZrTe_2$ were suspended in ACN at 5 µg/mL. Anhydrous conditions during perpetration and storage were maintained to minimize any solution instability or photo-hydrolytic degradation processes. The suspension was placed in a 1cm x 1cm cuvette, and excited by the second harmonic of a pulsed (532nm, 5Hz, 5ns) Nd:YAG laser. The excitation beam was incident on the cell at ~45 degrees angle of incidence (with respect to the cell front wall) and the emission was collected perpendicularly to the cell front wall. Reflections from the cuvette walls were avoided. The collected emission was directed to a spectrometer (Ocean Optics HR 4000), and the emitted intensity and bandwidth variation as a function of pump energy was obtained.

The typical characterization of random laser operation is shown in fig. 3, where the intensity emission and bandwidth reduction as a function of excitation energy are clearly seen for both bulk 3D $ZrTe_2$ particles (3a,b) and 2D exfoliated $ZrTe_2$ monolayers (3c,d). Figure 3a show the emission spectrum for a pulse excitation energy below the threshold (0.33 mJ) and another above the threshold (5.3 mJ) for which the narrowing of the full width at half maximum (FWHM). Figure 3b presents the bandwidth narrowing, characterized by the FWHM and the peak intensity as a function of the excitation pulse energy. For the 3D $ZrTe_2$ sample, the RL threshold can be determined from the emitted intensity slope, being approximately of 1.8 mJ.

Figures 3c and 3d show the same phenomenon described above, but for the 2D $ZrTe_2$ sample. It is also evident the decrease in the FWHM of the emission spectrum, although the narrowing reaches approximately 15 nm, instead of ~5nm observed for the powder case. The threshold in this case is approximately 1 mJ, which shows that the two-dimensional sample is somewhat more efficient than in the 3D case.

One important issue in RLs, particularly organic based RLs, is the useful lifetime, meaning the RL lifetime under pumping conditions above threshold. It has been seen in many publications that, due to chemical incompatibility between the organic dye and the scatterer. For instance, semiconductor nanoscatters, such as TiO_2, degrade organics via photocatalytic production of reactive oxygen species under hydrous conditions[39]. This photodegradation limits RL lifetime

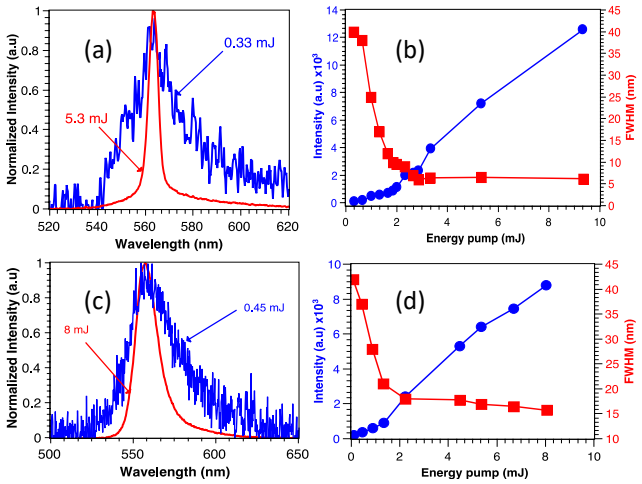

Fig. 3 RL characterization of the 3D $ZrTe_2$ particles and 2D exfoliated $ZrTe_2$. monolayers. (3a,c) shows the emission spectra for low energy and over the threshold for the 3D and 2D case respectively. (3a,d) shows FWHM and peak intensity of the emitted spectra as a function of the excitation energy for the 3D and 2D case respectively.

to just a few minutes under 5-10Hz repetition rate. There are ways to overcome this behavior, either managing the scattering material, as in ref.38 or using different gain-scatter combination, as in refs. 8,24,37. For example, semi-metals, such as $ZrTe_2$, do not photogenerate electron-hole pairs aligned with water's redox potential. Thus, photodegradation of the organic fluorophore (Rh6G) in the anhydrous $ZrTe_2$ suspensions will be suppressed, increasing the relative RL lifetime.

Figure 4 shows the results of the $ZrTe_2$ for both the 3D particles powder based RL (fig. 4a) and the 2D exfoliated monolayer based RL (fig. 4b), showing no photodegradation for over 90 min of continuous operation.

Due to its long term (several hours) lifetime and good shot-to-shot stability, we tested both $ZrTe_2$-based RL systems for observation of photonic paramagnetic-to-photonic spin-glass transition, similar to the work reported in [38], which followed the pioneer work of Ghofraniha and co-workers[36]. This is a phenomenon very characteristic of RL, and as mentioned before arises from a combination of scattering, multimode emission and gain, already observed in different RLs[40-43], besides the already referenced work[36-38]. Although this subject has been treated theoretically in early works[36,37,44], we summarize the main points here. In the laser physics context, each laser shot breeds a replica, which is a copy of the laser system emission - in this case the random laser - under very similar identical experimental conditions, provided the configurational disorder set by the random positions of the scatters does not change sensitively during the N_s laser shots. It can be shown that P(q), the probability density function (PDF), analogous to the Parisi order parameter in the RSB spin-glass theory[44], describes the distribution of replica overlaps $\boldsymbol{q} = \boldsymbol{q}_{\gamma\beta}$, therefore indicating a photonic paramagnetic or a RSB spin-glass phase, whether it peaks solely at $\boldsymbol{q} = \boldsymbol{0}$ (no RSB) or at values $|\boldsymbol{q}| \neq \boldsymbol{0}$ (RSB), respectively.

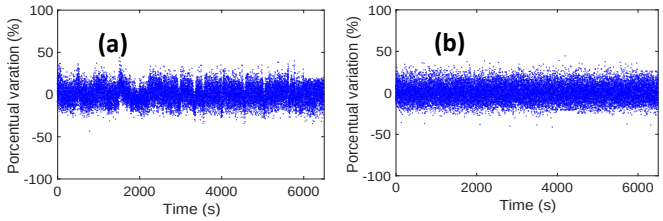

Fig. 4 Intensity behavior of the RL as a function of the time in seconds. The range of energy to which the 2D (fig.b) and 3D (fig.a) samples were exposed ranges from 300 $\boldsymbol{\mu J}$ to 10 mJ. No photodegradation was observed.

To characterize the transition from the fluorescent paramagnetic to the RL glassy behavior, an evaluation of the two-point correlation function that measures pulse-to-pulse fluctuations in the spectral intensity averaged over N_s laser shots at each pump energy is given by [36,38]:

$$q_{\gamma\beta} = \frac{\sum_k \Delta_\gamma(k)\Delta_\beta(k)}{\sqrt{\left[\sum_k \Delta_\gamma^2(k)\right]\left[\sum_k \Delta_\beta^2(k)\right]}}, \qquad (1)$$

where $\gamma, \beta = 1,2,\ldots,N_s$. The average intensity at the mode wavelength indexed by k reads $\bar{I}(k) = \sum_{\gamma=1}^{N_s} I_\gamma(k)/N_s$, and the intensity fluctuation is measured by $\Delta_\gamma(k) = I_\gamma(k) - \bar{I}(k)$. Taking into account that neither the nanoflakes or the powder in ACN solution did not photodegraded or precipitated during the experiment timeframe (~2 hour), one can consider the system conditions appropriate for the existence of replicas. Figure 5 shows the PDF $P(q)$ of both RL systems studied here, for N_s = 2000 shots.

The characteristic signature of both phases below and above threshold are seen in both 3D and 2D configurations (figs 5a-c and e-g respectively), and the calculated q_{max} in both cases show the phase-transition at the threshold values corresponding to the estimated before from fig. 3. The phase-transition is very distinct and the threshold values are quantitatively much better determined.

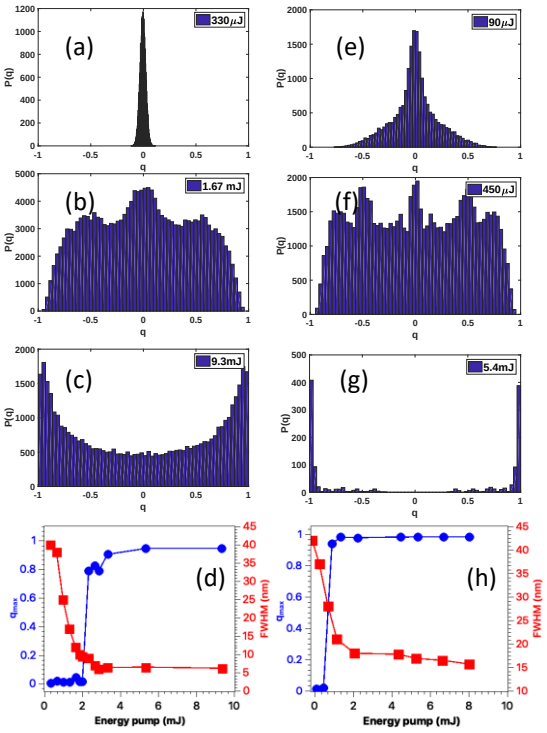

Fig. 5 Figures 5(a)–5(c) and 5(e)-5(g) display the PDF **P(q)** of the system for Ns = 2000 shots bulk powder 3D $ZrTe_2$ particles and 2D exfoliated $ZrTe_2$ monolayers RL respectively. Energies 330 μJ, 1.67 mJ and 9.3 mJ were chosen under, near and above the threshold to sample 3D. In the case 2D the energies shown are 90 μJ, 450 μJ and 5.4 mJ. Figure 5(d) and 5(h) shows q_{max} corresponding to the position of the maximum of P(|q|) versus pumping to 3D and 2D sample respectively.

Conclusions

In conclusion, we demonstrated random laser emission using 3D (powder) and 2D TMD $ZrTe_2$ nanoflakes as scatterers. We foresee further development of 2D based random lasers for photonics and optoelectronics applications. For example, the 2D TMD suspension-based random laser described here can be further exploited as platforms for flexible, stretchable random lasers[45], which employed perovskites as gain medium and graphene, graphene oxide or hexagonal boron nitride as scatters. As another example, the authors of ref.[46] employed inorganic Nd:YAB nanoparticles and polydimethylsiloxane to demonstrate stable elastomeric random laser emission, and similar devices can be exploited using 2D LTMDs. As a further example of such developments, with the advent of laser emission in 2D LTMDs using specially designed cavities (see ref. [47] for a review of light emission properties of 2D TMDS), the RL mechanism described here can be used to provide a simpler coherent light source based on 2D TMDs.

Conflicts of interest

There are no conflicts to declare.

Acknowledgements

The authors thank the financial support from the Brazilian Agencies CNPq, FACEPE, and CAPES. ASLG and MM acknowledge financial support from AFOSR. ASLG, MM, MLSN and CBA research was also supported within the framework of the National Institute of Photonics (CNPq/CAPES/FACEPE). AMJ, RB, AJR and RAV thank AFOSR and the Air Force Research Laboratory Materials and Manufacturing Directorate for financial support. Pablo I. R. Pincheira acknowledges support from FONDECYT No. 3180696.

References

1 N.M. Lawandy, R.M. Balachandran, A.S.L. Gomes, E. Sauvain, *Nature*, **1994**, 368, 436.
2 H. Cao, Y.G. Zhao, S.T. Ho, E.W. Seelig, Q.H. Wang, R.P.H. Chang, *Phys. Rev. Lett.* **1999**, 82, 2278.
3 Y.-C. Yao, Z.-P. Yang, J.-M. Hwang, H.-C. Su, J.-Y. Haung, T.-N. Lin, J.-L. Shen, M.-H. Lee, M.-T. Tsai, Y.-J. Lee, *Adv. Opt. Mater*. **2016**, 5, 1600746.
4 L. Sznitko, J. Mysliwiec, A. Miniewicz, *J. Polym. Sci., Part B: Polym. Phys*. **2015,** 53, 951.
5 A. L. Moura, S. I. Fewo, M. T. Carvalho, A. N. Kuzmin, P. N. Prasad, A. S. L. Gomes, and C. B. de Araújo, *J. Appl. Phys*. **2015**, 117 083102.
6 D. Zhang, G. Kostovski, C. Karnutsch and A. Mitchell, *Org. Electron*. **2012** 132342–5.
7 R.C. Polson, Z.V. Vardeny, *Appl. Phys. Lett*. **2004**, 85, 1289.
8 A. M. Brito-Silva, A. Galembeck, A. S. L. Gomes, A. J. Jesus-Silva, and C. B. de Araújo, *J. Appl. Phys*. **2010**, 108, 033508.
9 D. Cao, D. Huang, X. Zhang, S. Zeng, J. Parbey, S. Liu, C. Wang, T. Yi and T. Li, *Laser Physics*, **2018,** 28, 025801.
10 A. G. Ardakani and P. Rafieipour, *Physica B: Condensed Matter*, **2018**, 546, 49.
11 M.A. Noginov, *Solid-State Random Lasers*, Springer, New York, **2005**.
12 G.D. Dice, S. Mujumdar, A.Y. Elezzabi, *Appl. Phys. Lett*. **2005**, 86, 131105.
13 T. Zhai, Z. Xu, S. Li, and X. Zhang, *Opt. Express* **2017**, 25, 2100.
14 Y. Wan, Y. An and L. Deng, *Sci Rep.* **2017**, 7, 16185.
15 X.G. Meng, K. Fujita, S. Murai, T. Matoba, K. Tanaka, *Nano Lett*. **2011**,11, 1374.
16 C. J. S. de Matos, L. de S. Menezes, A. M. Brito-Silva, M. A. Martinez Gámez, A. S. L. Gomes and C. B. de Araújo, *Phys. Rev. Lett*. **2007**, 99, 153903-1/4.
17 M. Gagne´, R. Kashyap, *Opt. Express* **2009**, 17, 19067.
18 S.K. Turitsyn, S.A. Babin, A.E. El-Taher, P. Harper, D.V. Churkin, S.I. Kablukov, J.D. Ania-Castanon, V. Karalekas, E.V. Podivilov, *Nat. Photonics*, **2010**, 4, 231.

19 D. V. Churkin, S. Sugavanam, I. D. Vatnik, Z. Wang, E. V. Podivilov, S. A. Babin, Y. Rao, and S. K. Turitsyn, *Adv. Opt. Photon*. **2015**, 7, 516.
20 V.S. Letokhov, Zh. *Eksp. Teor.Fiz.* **1967**, 53, 1442 [Sov. Phys. JETP 26 (1968) 835-840].
21 F. Luan, B.Gu, A. S. L. Gomes, K.-T. Yong, S. Wen and P.N. Prasad, *Nano Today*, **2015**,10,168.
22 A. S. L. Gomes, *Nanocomposite-based random lasers: a review on basics and applications*, Ch. 3 in Nanocomposites for Photonic and Electronic Applications, Edited by L. R. P. Kassab, S. J.L. Ribeiro and R. Rangel-Rojo, Elsevier, 2020.
23 D.S. Wiersma, The physics and applications of random lasers, *Nat. Phys*. **2008**, 4, 359.
24 H.Cao, *J. Phys. A: Math. Gen*. **2005**, 38, 10497.
25 N. Huo, Y. Yang, J. Li. *J. Semicond*. **2017,** 38, 031002-1/9.
26 A. Autere, H. Jussila, Y. Dai, Y. Wang, H. Lipsanen, Z. Sun. *Adv. Mater*. **2018**, 30, 1705963.
27 R. Kurapati, K. Kostarelos, M. Prato, A. Bianco. *Adv. Mater*. **2016**, 28, 6052.
28 Z. Wei, B. Li, C. Xia, Y. Cui, J. He, J.-B. Xia, J. Li. *Small Methods*. **2018**, 2 1800094.
29 W. Choi, N. Choudhary, G. Han Hee, J. Park, D. Akinwande, Y.H. Lee. *Materials Today* **2017**, 20, 116.
30 A. Jawaid, J, Che, L. F.Drummy, J. Bultman, A. Waite, M. S. Hsiao, R. A. Vaia. *ACS Nano*. **2017,** 11, 635.
31 P. Ren, W. Zhang, Y.Ni, D. Xiao, H. Wan, Y.-P. P. L. Li, P. Yan and S. Ruan, *Nanomaterials*, **2018**, 8, 538;
32 O. Salehzadeh, M. Djavid, N. H. Tran, I. Shih, and Z. Mi. *Nano Lett*. **2015**, 15, 5302.
33 L. Reeves, Y. Wang, and T. F. Krauss, *Adv. Optical Mater*. **2018** 6, 1800272
34 T. Dixit, A. Arora, A. Krishnan, K. L. Ganapathi, P. K. Nayak and M. S. R. Rao, *ACS Omega,* **2018**, 3, 14097.
35 S A O'Brien, A Harvey, A Griffin, T Donnelly, D Mulcahy, J N Coleman, J F Donegan and D McCloskey, *Nanotechnology,* **2017**, 28 47LT02 (7pp)
36 N. Ghofraniha, I. Viola, F. Di Maria, G. Barbarella, G. Gigli, L. Leuzzi, and C. Conti, *Nat. Commun*. **2015**, 6, 6058.
37 A. S. L. Gomes, E.P. Raposo, A. L. Moura, S. I. Fewo, P.I. R. Pincheira, V. Jerez, L. J. Q. Maia, and C. B. de Araújo, *Sci. Rep*. **2016**, 6, 27987.
38 P. I. R. Pincheira, A. F. Silva, S. J. M. Carreño, S. I. Fewo, A. L. Moura, E. P. Raposo, A. S. L. Gomes and C. B. de Araújo, *Opt. Lett*. **2016**, 41, 3459.
39 M. Pawar , S. T. Sendoğdular and P. Gouma , Journal of Nanomaterials **2018,** Article ID 5953609, 13 pages.
40 A. S. L. Gomes, B. C. Lima, P. I. R. Pincheira, A. L. Moura, M. Gagné, E. P. Raposo, C. B. de Araújo, and R. Kashyap, *Phys. Rev. A*, **2016**, **94,** 011801(R).
41 F. Tommasi, E. Ignesti, S. Lepri, and S. Cavalieri, *Sci. Rep*. **2016,** 6, 37113.
42 A. Sarkar, J. Andreasen, and B. B. N. Shivakiran, *Frontiers in Optics*, **2017**, JW3A.30.
43 J. Xia, J. He, K. Xie, X. Zhang, L. Hu, Y. Li, X. Chen, J. Ma, J. Wen, J. Chen, Q. Pan, J. Zhang, I. D. Vatnik, D. Churkin, Z. Hu, *Ann. Phys*. **2019**, 531, 1900066.
44 M. Mézard, G. Parisi, and M. A. Virasoro, *Spin Glass Theory and Beyond*. World Scientific, vol. 9, **1987**.
45 H.-W. Hu, G. Haider, Y.-M. Liao, P. K. Roy, R. Ravindranath, H.-T. Chang, C.-H. Lu, C.-Y. Tseng, T.-Y. Lin, W.-H. Shih, and Y.-F. Chen, *Adv. Mater*. **2017**, 1703549
46 A.R. Hlil, B.C. Lima, J. Thomas, J-S. Boisvert, H. Iden, Y. Garcia-Puente, L.J.Q. Maia, Y. Ledemi, Y. Messaddeq, A. S. L. Gomes and R. Kashyap, *Opt. Mater.* **2019**, 97, 109387.
47 W. Zheng, Y. Jiang, X. Hu, Honglai Li, Z. Zeng, X. Wang and A. Pan, Adv. Optical Mater. **2018**, 1800420, 1-29.